ORIGINAL ARTICLE

JBMR®

Lipocalin 2: A New Mechanoresponding Gene Regulating Bone Homeostasis

Nadia Rucci,[1] Mattia Capulli,[1] Sara Gemini Piperni,[1] Alfredo Cappariello,[2] Patrick Lau,[3] Petra Frings-Meuthen,[3] Martina Heer,[4] and Anna Teti[1]

[1]Department of Biotechnological and Applied Clinical Sciences, University of L'Aquila, L'Aquila, Italy
[2]Bambino Gesù Children Hospital, "Istituto di Ricovero e Cura a Carattere Scientifico" (IRCCS), Rome, Italy
[3]German Aerospace Center (DLR), Institute of Aerospace Medicine, Cologne, Germany
[4]Department of Nutrition and Food Science, Nutritional Physiology, University of Bonn, Germany

ABSTRACT

Mechanical loading represents a crucial factor in the regulation of skeletal homeostasis. Its reduction causes loss of bone mass, eventually leading to osteoporosis. In a previous global transcriptome analysis performed in mouse calvarial osteoblasts subjected to simulated microgravity, the most upregulated gene compared to unit gravity condition was *Lcn2*, encoding the adipokine Lipocalin 2 (LCN2), whose function in bone metabolism is poorly known. To investigate the mechanoresponding properties of LCN2, we evaluated LCN2 levels in sera of healthy volunteers subjected to bed rest, and found a significant time-dependent increase of this adipokine compared to time 0. We then evaluated the in vivo LCN2 regulation in mice subjected to experimentally-induced mechanical unloading by (1) tail suspension, (2) muscle paralysis by botulin toxin A (Botox), or (3) genetically-induced muscular dystrophy (MDX mice), and observed that *Lcn2* expression was upregulated in the long bones of all of them, whereas physical exercise counteracted this increase. Mechanistically, in primary osteoblasts transfected with LCN2-expression-vector (OBs-Lcn2) we observed that *Runx2* and its downstream genes, *Osterix* and *Alp*, were transcriptionally downregulated, and alkaline phosphatase (ALP) activity was less prominent versus empty-vector transduced osteoblasts (OBs-empty). OBs-Lcn2 also exhibited an increase of the *Rankl/Opg* ratio and *IL-6* mRNA, suggesting that LCN2 could link poor differentiation of osteoblasts to enhanced osteoclast stimulation. In fact, incubation of purified mouse bone marrow mononuclear cells with conditioned media from OBs-Lcn2 cultures, or their coculture with OBs-Lcn2, improved osteoclastogenesis compared to OBs-empty, whereas treatment with recombinant LCN2 had no effect. In conclusion, our data indicate that LCN2 is a novel osteoblast mechanoresponding gene and that its regulation could be central to the pathological response of the bone tissue to low mechanical forces. © 2014 American Society for Bone and Mineral Research.

KEY WORDS: LCN2; ADIPOKINE; MECHANICAL FORCES; UNLOADING; OSTEOCLASTS; OSTEOBLASTS

Introduction

Lipocalin 2 (LCN2), also known as 24p3 and Neutrophil Gelatinase-Associated Lipocalin (NGAL),[1,2] is a 25-kD adipokine belonging to a large superfamily of proteins that bind and transport lipids and other hydrophobic molecules. Consistent with its expression in several cell types and organs, including neutrophils, adipocytes, macrophages, liver, and kidney, LCN2 is implicated in diverse functions. For instance, it takes part in the host innate immune response through its bacteriostatic effect induced by the binding of bacterial siderophores, which limits bacterial iron acquisition.[3] Accordingly, LCN2-deficient mice are more sensitive to certain Gram-negative bacteria and die more readily of sepsis compared to WT mice.[4,5]

Recently, a role of LCN2 in energy metabolism has been shown; this protein is highly expressed in the adipose tissue and circulating LCN2 levels are increased in obese animals and in patients with type 2 diabetes.[6,7] Moreover, serum concentrations of LCN2 are positively associated with waist circumference, percent of body fat, systolic blood pressure, fasting glucose and insulin concentrations, fasting triglycerides, and markers of chronic inflammation.[6] Serum LCN2 levels are also elevated in patients with coronary heart disease and are associated with atherosclerosis.[8] Furthermore, the expression of LCN2 rises 1000-fold in humans and rodents in response to renal tubular

Received in original form January 23, 2014; revised form July 29, 2014; accepted August 5, 2014. Accepted manuscript online August 12, 2014.
Address correspondence to: Anna Teti, PhD, Department of Biotechnological and Applied Clinical Sciences, Via Vetoio – Coppito 2, 67100 L'Aquila, Italy.
E-mail: teti@univaq.it
*NR and MC contributed equally to this work.
Public clinical trial registration: http://clinicaltrials.gov/show/NCT01183299. Influence of a High Salt Intake on Sodium Retention, Bone Metabolism and Acid-base Balance in Immobilised Test Subjects.
Additional Supporting Information may be found in the online version of this article.
Journal of Bone and Mineral Research, Vol. 30, No. 2, February 2015, pp 357–368
DOI: 10.1002/jbmr.2341

injury, and it appears so rapidly in urine and serum that it is proposed to be an early biomarker of renal failure.[9]

So far, two LCN2 cell-surface receptors have been identified. One receptor, called 24p3R (alluding to LCN2's original name, 24p3), is a protein that originally was referred to as brain organic cation transporter, which is a membrane-associated protein with 12 predicted transmembrane helices.[10] A second LCN2 receptor is the well-characterized multiprotein receptor megalin-cubilin,[11] expressed by kidney proximal tubule cells, which are known target cells of LCN2.[12]

Despite the several recognized functions accomplished by CN2 in different tissues under physiologic and pathologic conditions, there are many questions still unsolved about the role of this molecule in the body. Because the function of LCN2 in bone homeostasis is barely known, we sought to investigate its involvement in this context based on a previous work in which we demonstrated that LCN2 could be a mechanoresponding gene that correlated with poor osteoblast activity.[13] In fact, in a global transcriptome analysis of mouse calvarial osteoblasts grown for 5 days under modeled microgravity (0.08*g* and 0.008*g*) to simulate low mechanical loading, we evidenced modulation of transcripts involved in osteoblast differentiation, as well as changes in the expression of a set of genes not previously correlated with bone metabolism, among which the most upregulated gene was *Lcn2*.[13]

Based on this evidence, the aim of this study was to investigate the role of LCN2 in depth in the response of bone to mechanical unloading in vivo and in vitro. We showed that LCN2 is upregulated in human and animal models of reduced mechanical forces, and identified the cellular mechanisms underlying its effects on osteoblasts and osteoclasts.

Materials and Methods

Materials

Dulbecco's modified minimum essential medium (DMEM), fetal bovine serum (FBS), penicillin, streptomycin, and trypsin were from GIBCO (Uxbridge, UK). Sterile plastic ware was from Falcon Becton-Dickinson (Cowley, Oxford, UK) or Costar (Cambridge, MA, USA). Trizol reagent, primers, and reagents for RT-PCR were from Invitrogen (Carlsbad, CA, USA). The Brilliant SYBR Green QPCR master mix was from Stratagene (La Jolla, CA, USA). Human recombinant (hr) receptor activator of nuclear factor κ-light-chain-enhancer of activated B cells transcription factor ligand (RANKL) (#310-01) and hr macrophage–colony stimulating factor (M-CSF) (#300-25) were from Peprotech EC (London, UK). Anti-megalin antibody (cat# sc-16478) was from Santa Cruz Biotechnology, Inc. (Santa Cruz, CA, USA); anti-LCN2 antibody (cat# AF1857), mouse recombinant (mr) Lipocalin2 (cat# 1857-LC-050), and human ELISA kit for LCN2 (DLCN20) were purchased from R&D Systems Inc. (Minneapolis, MN, USA). All the other reagents were of the purest grade from Sigma Aldrich Co. (St. Louis, MO, USA).

Ethics

Approval for the study was obtained from the Ethical Committee of the "Aerztekammer Nordrhein," Düsseldorf, Germany, and was conducted in accordance with the latest version of the Declaration of Helsinki. The study is registered on http://www.clinicaltrials.gov with the unique trial number: NCT01183299; registration date: August 13, 2010.

Protocol for the human study

The primary focus of this bed rest study was to test if low-grade metabolic acidosis induced by high NaCl intake exacerbates bone resorption during immobilization. For this reason, a 14-day head-down tilt bed rest (HDBR) study, including 8 male test subjects (mean age 26.3 ± 3.5 years, body weight [BW] 78.0 ± 4.3 kg) was conducted in the metabolic ward of the German Aerospace Center. Immobilization was accomplished with 6-degree HDBR, a valid ground-based model to simulate microgravity-induced bone loss.[14] During the bed rest period the subjects received in a crossover design either a high (7.7 mEq/kg BW per day) or a low (0.7 mEq/kg BW per day) NaCl diet. The two parts of the study were performed separately with a 6-month washout period in between. Study design and primary outcome are described more detailed in Frings-Meuthen and colleagues.[14] For the assessment of serum LCN2 levels in the present study, we took advantage of unutilized study samples.

Blood sampling and analysis

Blood samples were drawn on day 0 just before confinement to bed and during bed rest on days 4, 6, 8, 11, and 15. Blood samples were obtained by venipuncture from a forearm vein and collected into 5-mL serum separator tubes. After centrifugation, serum samples were aliquoted into 1-mL cryotubes and kept frozen at −80°C until use. LCN2 concentration was measured using a commercially available ELISA kit according to the manufacturer's recommendations.

Animals

Procedures involving animals care were conducted in conformity with national and international laws and policies (EEC Council Directive 86/609, OJ L 358, 1, Dec. 12, 1987; Italian Legislative Decree 116/92, *Gazzetta Ufficiale della Repubblica Italiana* n. 40, Feb. 18, 1992; NIH guide for the Care and Use of Laboratory Animals, NIH Publication No. 85-23, 1985), and were approved by the Institutional Review Board of the University of L'Aquila. At the end of the experiments, mice were euthanized by CO_2 inhalation. All experiments were performed in female mice. Key experiments repeated in male mice showed similar results (not shown).

Hindlimb suspension

Hindlimb suspension was obtained according to Sakata and colleagues[15] on 8-week-old C57BL/6 mice. A strip of elastic tape forming a half-circle at the center of the tail was applied to the ventral surface of the tail. A swivel attached to the half-circle of tape was fixed to an overhead wire, the height of which was adjusted to maintain the mice suspended at an approximately 30-degree angle. The swivel apparatus allowed animals ready access to food and water and to move freely into the cage using their forelimbs. After 21 days of suspension mice were euthanized by CO_2 inhalation, hindlimbs were removed and cleaned from soft tissues, then they were frozen in dry ice and subjected to RNA extraction. An equal number of mice was maintained under normal cage conditions for 21 days as control.

In vivo treatment with botulin toxin A

Eight-week-old C57BL/6 mice were subjected to botulin toxin A (Botox) injection according to Warner and colleagues.[16] Briefly, mice were anesthetized, then the left and the right hindlimbs of each mice were injected with saline solution (20 μL) and with

Botox (2.0 unit/100 g), respectively, into the right quadriceps and the posterior compartment of the right calf (targeting gastrocnemius, plantaris, and soleus). The behavioral response of each mouse was quantified on days 1, 3, 7, and weekly thereafter using whole body weight measurement and assessment of gait disability. After 21 days mice were sacrificed, then the hindlimbs were removed, femurs and tibias were cleaned free of soft tissues and frozen in dry ice or fixed in 4% buffered paraformaldehyde for RNA extraction and morphometric analysis of bone parameters, respectively.

MDX mice

Eight-week-old X chromosome-linked muscular dystrophy (MDX) homozygous mice (CB6F1/C57BL6 background) carrying a spontaneous single-base mutation on exon 23 of the dystrophin gene[17,18] were used for analysis of the bone phenotype and for mRNA expression of LCN2 in tibias. Age-matched normal mice of the same background were employed as controls. Mice were euthanized by CO_2 inhalation, and hindlimb bones were excised, cleaned of soft tissues, frozen in dry ice, and processed for RNA extraction.

Treadmill exercise

WT and MDX mice were enforced to run on a mobile platform at a speed of 9 m/min for 30 min, twice a week for 3 weeks. Because mice carried muscular dystrophy, to avoid excessive stress due to increasing running time, physical exercise was not progressive.

Forced swimming test

WT mice subjected to hindlimb suspension were forced to swim in a 250-L water-filled tank (water depth = 20 cm), with water temperature kept at 31 °C. This test lasted 5 min and was repeated 3 times/day for 3 days/week during the entire period of unloading (3 weeks).[19] Control mice were left for the same time of swimming test under unloading conditions.

Micro–computed tomography analysis

Tibias were mounted and acquired in a SkyScan 1174 micro–computed tomography (μCT) scanner, with a voxel size of 6 μm (X-ray voltage 50 kV). Image reconstruction was carried out employing a modified Feldkamp algorithm using the Skyscan Nrecon software. Beam hardening correction and Fourier transform–based ring artifact reduction were applied to the reconstructed images. 3D and 2D morphometric parameters were calculated for the trabecular bone of selected regions of interest, 150 slides, 400 μm from the growth plate. Threshold values were applied for segmenting trabecular bone corresponding to bone mineral density values of 0.6/cm^3 calcium hydroxyapatite. 3D parameters were based on analysis of a Marching Cubes type model with a rendered surface.[20] Calculation of 2D areas and perimeters was based on the Pratt algorithm. Bone structural variables and nomenclature were those suggested in Bouxsein and colleagues.[21]

Bone histomorphometry

Tibias fixed in 4% paraformaldehyde were dehydrated in acetone and processed for glycol–methacrylate embedding without decalcification. Histomorphometric measurements were carried out on 5-μm-thick sections with an interactive image analysis system (IAS 2000; Delta Sistemi, Rome, Italy)[22] and with the suggested nomenclature.[23] Osteoclast surface/bone surface (%) was evaluated after histochemically staining the sections for tartrate-resistant acid phosphatase (TRAcP) activity. Osteoblast surface/bone surface (%) was evaluated after staining the sections with methylene blue/azure II.

Bone biomechanical properties

Explanted femurs were cleaned out of soft tissues and stored at –80°C. They were then thawed in ice and soaked in ice-cold PBS. The analysis was performed on the distal portion of the femur using Reference Point Indentation (Biodent Hfc, Active Life Scientific, Santa Barbara, CA, USA). Samples were tested using the test probe BP2 and the following parameters: 10 indentation cycles at 2 Hz to a force of 4 N. Bones were maintained in an hydrated state throughout the test. Total indentation distance and total energy dissipation were calculated for each test. Five tests from each animal were averaged to produce a single value for each variable.

Calvarial osteoblast cultures

Calvariae from 7-day-old CD1 mice were removed, cleaned free of soft tissues, and digested three times with 1 mg/mL *Clostridium histolyticum* type IV collagenase and 0.25% trypsin, for 20 min at 37°C with gentle agitation. Cells from the second and third digestions were plated and grown in standard conditions, in DMEM plus 10% FBS. At confluence, cells were trypsinized by standard procedures and plated according to the experimental protocol. These cells expressed the osteoblast markers ALP, Runx-2, parathyroid hormone (PTH)/PTH related peptide receptor, type I collagen, and osteocalcin.

Alkaline phosphatase activity assay

Primary mouse osteoblasts were fixed in 4% paraformaldehyde for 15 min, then washed with PBS. Alkaline phosphatase (ALP) activity was evaluated histochemically using the Sigma-Aldrich kit n. 85, according to the manufacturer's instruction. Quantitative analysis was performed by scanning densitometry using the Molecular Analyst software for the model 670 scanning densitometer (Bio-Rad Laboratories, Hercules, CA, USA) to obtain arbitrary density units.

Amaxa Nucleofector transfection

Primary mouse osteoblasts (1×10^6) were nucleofected with 2 μg of empty or LCN2-carrying pCMV-3TAG8 vectors, using the Amaxa Mouse Neuron Nucleofector kit (Lonza, Basel, Switzerland; Cat. VPG-1001) and the program T-030 of the nucleofector device. After 48 hours from nucleofection, osteoblasts were employed for the experiments.

Osteoclast primary cultures

Bone marrow flushed out from the bone cavity of the long bones of 7-day-old CD1 mice was diluted 1:1 in Hank's balanced salt solution, layered over Histopaque 1077 solution and centrifuged at 400*g* for 30 minutes. Cells were washed twice with Hank's solution, resuspended in DMEM, and plated in culture dishes at a density of 10^6 cells/cm^2. After 3 hours, cell cultures were rinsed to remove nonadherent cells and maintained for 7 days in the same medium supplemented with 50 ng/mL rhM-CSF and suboptimal concentrations of rhRANKL (30 ng/mL), plus 100 ng/mL rmLCN2 or undiluted conditioned media from osteoblasts overexpressing LCN2 or transfected with an empty vector as control.

Osteoblast-osteoclast cocultures

Primary mouse osteoblasts, transfected by the Amaxa method with the LCN2 vector or with an empty vector, were plated in 48-well plates. When cells reached 30% confluence, purified mouse bone marrow mononuclear cells, obtained by the protocol described in the previous section (osteoclast primary culture) were added to the osteoblast cultures at a density of 1×10^6 cells/mL. After 7 days of coculture, osteoclasts were detected by TRAcP histochemical staining.

TRAcP activity assay

Cells were fixed in 4% paraformaldehyde for 15 min, then extensively washed with the same buffer. TRAcP activity was detected histochemically, using the Sigma-Aldrich kit# 386, according to the manufacturer's instruction.

Immunohistochemistry

Tibias were cleaned free of soft tissues and fixed with 4% paraformaldehyde for 48 hours, then decalcified in Osteodec (Bio-Optica, Milan, Italy) for further 48 hours and embedded in paraffin to obtain 5-μm-thick sections. Sections were then deparaffinized, incubated with 0.07 M citrate buffer (pH 6) for 15 min at 98 °C for antigen retrieval, treated with 3% H_2O_2, and incubated overnight at 4 °C with the anti-Lcn2 mouse monoclonal antibody. The staining signal was revealed using the Dako LSAB System-HRP (Dako North America, Inc., Carpinteria, CA, USA; cat# K0679) following the manufacturer's instructions. Negative controls (omitting the primary antibody) were performed in parallel.

Immunofluorescence

Mouse primary osteoblasts were fixed with 4% paraformaldehyde and incubated for 1 hour at room temperature with specific primary antibodies followed by FITC-conjugated secondary antibody or tetramethylrhodamine isothiocyanate (TRITC)-conjugated secondary antibody. To detect nuclei, cells were stained with 4,6-diamidino-2-phenylindole (DAPI). Cells were then observed at room temperature by conventional epifluorescence (Axioplan; Carl Zeiss, Inc., Thornwood, NY, USA) confocal (FluoView IX81 FVBF; Olympus, Tokio, Japan) microscope. For fluorescence microscopy, we used 2.5× NA 0.075, 10× NA 0.30, 20× NA 0.5, and 40× NA 0.75 Plan-Neofluar objective lenses. Images were captured with a camera (AxioCam MRC5; Carl Zeiss, Inc.) using the AxioVs 40 version 4.7.1.0 software (Carl Zeiss, Inc.). For confocal microscopy, we used 10× NA 0.30 and 40× NA 0.85 UPlan-Apochromat or 60× NA 1.4 oil Plan-Apochromat objective lenses. Images were captured using FluoView 500 software (Olympus).

HEK293 cells

The HEK293 cell line was obtained from the American Tissue Culture Collection (ATCC, Rockville, MD, USA), and grown in DMEM supplemented with 10% FBS, 100 IU/mL penicillin, 100 μg/mL streptomycin, and 2 mM L-glutamine. Cells were grown in a 5% CO_2 humidified atmosphere at 37°C.

To overexpress LCN2, HEK293 cells were transiently transfected with the pCMV-3TAG8 expression vector containing LCN2, using Lipofectamine and PLUS reagent. Control transfectants were obtained by transfecting HEK293 cells with an empty pCMV-3TAG8.

Semiquantitative and comparative real-time RT-PCR

Total RNA was extracted from mouse whole femurs or from osteoblasts using the Trizol procedure. RNA (1 μg) was reverse transcribed in cDNA using M-MLV reverse transcriptase and the equivalent of 0.1 μg was employed for the real-time PCR reactions using Brilliant SYBR Green QPCR master mix or for semiquantitative PCR. PCR conditions and primer pairs are listed in Table 1. Results, expressed as fold increase for real-time RT-PCR, or shown by electrophoresis of PCR products in a 2% agarose gel plus ethidium bromide for conventional RT-PCR, were normalized versus the housekeeping gene *Gapdh*.

Statistics

Results are expressed as the mean ± SD of at least three independent experiments, 8 human subjects, and at least 3 mice/group. Statistical analyses were performed by the Student's *t* test, the linear regression test or the nonparametric Mann-Whitney rank sum test, according to the type of data sets. The statistical methods are indicated in the figure legends. A p value <0.05 was conventionally considered statistically significant.

Results

LCN2 expression in sera of patients subjected to prolonged bed rest

In our previous study we demonstrated that *Lcn2* is a mechanoresponding gene, upregulated in mouse primary osteoblasts by mechanical unloading simulated in the NASA-developed rotating wall vessel bioreactor by reducing the gravitational forces.[13] Based on these data, we evaluated LCN2 in healthy volunteers, subjected to HDBR, an analogue model used to mimic microgravity-induced bone and muscle loss. This trial was originally designed to investigate the association between high NaCl intake, concomitant with a low-grade

Table 1. Primer Pairs Employed for Comparative Real-Time and Semiquantitative RT-PCR

Gene	Forward primer	Reverse primer
GAPDH	5′-TGGCAAAGTGGAGATTGTTGC-3′	5′-AAGATGGTGATGGGCTTCCCG-3′
Lcn 2	5′-CCAGTTCGCCATGGTATTTT-3′	5′-CACACTCACCACCCATTCAG-3′
Alp	5′-CCAGCAGGTTTCTCTCTTGG-3′	5′-CTGGGAGTCTCATCCTGAGC-3′
Runx2	5′-AACCCACGGCCCTCCCTGAACTCT-3′	5′-ACTGGCGGGGTGTAGGTAAAGGTG-3′
Osterix	5′-TGCTTCCCAATCCTATTTGC-3′	5′-AGAATCCCTTTCCCTCTCCA-3′
IL-6	5′-GAGGATACCACTCCCAACAGACC-3′	5′-AAGTGCATCATCGTTGTTCATACA-3′
RankL	5′-CCAAGATCTCTAACATGACG-3′	5′-CACCATCAGCTGAAGATAGT-3′
Opg	5′-AAAGCACCCTGTAGAAAACA-3′	5′-CCGTTTTATCCTCTCTACACTC-3′

PCR conditions were 94°C for 30 s, 60°C for 30 s, and 72°C for 30 s, replicated for 40 cycles for real-time RT-PCR and 27 cycles for semiquantitative RT-PCR.

metabolic acidosis, and exacerbated bone resorption and protein wasting.[14] We took advantage of unutilized study samples and found that the serum LCN2 levels were higher after HDBR if compared to basal levels (time 0) (Fig. 1), revealing direct correlation between LCN2 levels and time of HDBR. Changes were not associated to sodium intake as suggested by the lack of statistical significance between the low (Fig. 1, black symbols) and the high (Fig. 1, open symbols) sodium intake groups at each time point. Induction of LCN2 was progressive and achieved statistical significance after 12 days of HDBR (Fig. 1). In agreement with our previous in vitro findings, that demonstrated an increase of LCN2 in primary osteoblasts picking after 5 days of unloading,[13] we can conclude that LCN2 induction is not an early event as it requires days of stimulation by decreased mechanical forces.

LCN2 expression in the bones of animal models subjected to unloading condition

The evidence in humans, together with the in vitro results previously obtained in isolated murine osteoblasts,[13] prompted us to further characterize the relationship between *Lcn2* expression and the response of bone to reduced mechanical forces in animal models. We first employed the tail suspension of mice as a model of hindlimb unloading[15] and found that the mRNA expression of *Lcn2* significantly increased in the bones of the suspended hindlimbs with respect to those of the hindlimbs of mice maintained under normal conditions, employed as controls (Fig. 2*A*). Noteworthy, this increase was antagonized by physical exercise through the forced swimming test (Fig. 2*A*).

To identify the cell lineage producing more LCN2 in tail suspended mice, we performed a FACS analysis of bone marrow cells flushed out from femurs. We found that the $CD45^-$ subpopulation, known to represent the bone marrow stromal cells and to include the osteoblast lineage, was the only one responding to the unloading conditions by increasing its LCN2 expression.

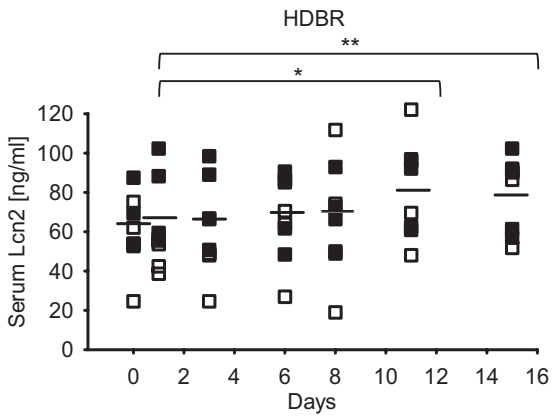

Fig. 1. LCN2 expression in sera of patients subjected to prolonged HDBR. An ELISA assay for human LCN2 performed in sera of 8 healthy volunteers subjected to HDBR (15 days). Sera were collected just before the HDBR (day 0) and during the HDBR (days 1, 3, 6, 8, 11, 15). Open squares: 500 mmol NaCl/day, black squares: 50 mmol NaCl/day. $^*p = 0.003$ and $^{**}p = 0.001$ versus day 0; differences between 500 mmol NaCl/day and 50 mmol NaCl/day are statistically not significant, with $p > 0.21$ (paired *t* test). HDBR = head-down tilt bed rest.

This increase was again antagonized by the physical exercise (Fig. 2*B*).

Next, we asked whether the biomechanical properties of the bones of these mice, known to be impaired by unloading (Fig. 2*C*, *D*), correlated with the *Lcn2* modulation. Indeed, the regression test showed a direct correlation between *Lcn2* transcriptional expression and the total indentation distance (Fig. 2*E*), a parameter that increases when the bone quality is compromised.

We have previously reported that dystrophic homozygous *MDX* mice[17] are characterized by an osteopenic phenotype.[18] In these mice we analyzed the *Lcn2* mRNA expression in bone and, consistent with the results of hindlimb suspension, we observed that it was significantly increased with respect to the WT littermates (Fig. 2*F*). This increase was prevented subjecting the MDX mice to physical exercise by treadmill running (Fig. 2*F*).

We next created an additional model of mechanical unloading injecting Botox in both quadriceps and calf muscles of the right hindlimbs of 5-week-old mice. This procedure induced a transient paralysis causing a dramatic alteration of muscle organization, as demonstrated by hematoxylin/eosin staining of muscle sections (Fig. 3*A*). As expected,[16] this mechanical impairment induced a reduction of bone volume/total tissue volume (Fig. 3*B*) and trabecular number (Fig. 3*C*), no modulation of trabecular thickness (Fig. 3*D*), and an increase of trabecular separation (Fig. 3*E*). Histomorphometric analysis revealed an increase of osteoclast surface (Fig. 3*F*), together with a decrease of osteoblast surface (Fig. 3*G*) over bone surface and a trend of increase of bone marrow adiposity (Fig. 3*H*, *I*). Again, under this loading constraint we observed a significant increase of LCN2 both at the protein (Fig. 4*A*) and transcriptional (Fig. 4*B*) level. Consistently, serum level of LCN2 was time-dependently increased in Botox-treated mice compared to control mice (Fig. 4*C*). Biomechanical tests confirmed impaired mechanical properties induced by unloading (Fig. 4*D*, *E*), whereas regression tests evidenced that *Lcn2* mRNA level had a direct correlation with the reduction of mechanical strength (Fig. 4*F*) and an inverse correlation with the bone volume/total tissue volume (Fig. 4*G*).

To address whether high *Lcn2* levels were involved in bone mass loss also independently of mechanical unloading, we evaluated *Lcn2* expression in ovariectomized (OVX) mice and observed that, in this circumstance, *Lcn2* expression was significantly reduced both at transcriptional and protein level compared to sham-operated mice (Supporting Fig. 1A, B). This result suggests that LCN2 overexpression represents a specific response of bone to mechanical release.

Role of LCN2 in osteoblast activity

To dissect the role of LCN2 in osteoblast metabolism, mouse primary osteoblasts were transfected with *Lcn2*-expression-vector (OBs-LCN2) or with control empty vector (OBs-empty). Successful overexpression of LCN2 was confirmed at mRNA (Fig. 5*A*) and protein (Fig. 5*B*) levels by real-time RT-PCR and ELISA assays, respectively. Interestingly, OBs-LCN2 exhibited a less differentiated phenotype, as indicated by a lower transcriptional expression of *Alp* (Fig. 5*C*), *Runx2* (Fig. 5*D*), and *Osterix* (Fig. 5*E*) genes, compared to OBs-empty. Consistently, histochemical evaluation of ALP evidenced a lower activity in OBs-LCN2 versus OBs-empty (Fig. 5*F*). Primary osteoblasts transfected with *Runx2* expression vector (Supporting Fig. 2A) showed no change of *Lcn2* transcriptional level (Supporting Fig. 2B), implying that *Lcn2* is likely to represent a primary

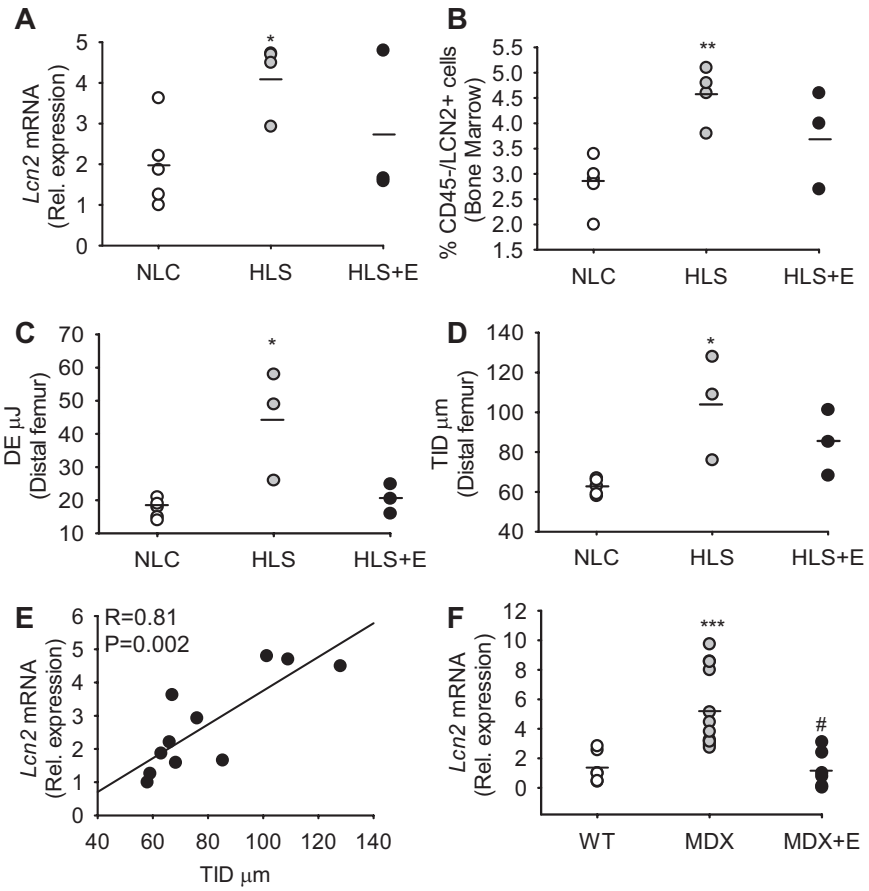

Fig. 2. Effect of in vivo mechanical unloading on LCN2 expression. Eight-week-old mice were maintained in NLC or were subjected to HLS for 21 days. A group of them was subjected to physical exercise (HLS + E) (forced swimming test) during the experiment of unloading, as described in Materials and Methods. (*A*) Transcriptional evaluation of *Lcn2* expression in the hindlimb bones by comparative real-time RT-PCR. (*B*) Evaluation by FACS analysis of the percent of $CD45^{-}/LCN2^{+}$ cells in the bone marrow. (*C*) DE (μJ) and (*D*) TID (μm) in distal femurs. (*E*) Linear regression test showing a direct correlation between *Lcn2* mRNA and distal femoral TID. Data are the mean ± SD. $^{*}p < 0.038$ and $^{**}p = 0.016$ versus NLC (nonparametric Mann-Whitney rank sum test). (*F*) Transcriptional expression of *Lcn2* by comparative real-time RT-PCR in 8-week-old WT and MDX (X chromosome-linked muscular dystrophy) mice, the latter maintained under sedentary conditions or subjected to physical exercise (MDX + E) (treadmill running). $^{***}p = 0.001$ versus WT and $\#p = 0.002$ versus MDX (nonparametric Mann-Whitney rank sum test). NLC = normal loading conditions; HLS = hindlimb suspension; DE = dissipated energy; TID = total indentation distance.

osteoblast gene not subjected to *Runx2* regulation. Finally, in OBs-LCN2 we observed an increase of phosphorylated ERK, suggesting the involvement of the MAPK pathway in the LCN2 signaling (Fig. 5*G*). Accordingly, osteoblasts expressed both LCN2 receptors, 24p3R and megalin (Fig. 5*H*, *I*) which, however, were not modulated during osteoblast differentiation as demonstrated by the lack of correlation with the osteoblast differentiating genes *Alp* and *Runx2*, and with *Lcn2* itself (Supporting Fig. 2C). These results support a dominant role of LCN2 in causing the poor osteoblast differentiation observed in our previous study performed under simulated microgravity[24] and underscore the involvement of a receptor-mediated mechanism associated to the ERK pathway.

Role of LCN2 on osteoclast activity

Because osteoblasts are the main players in the regulation of osteoclast formation and function, we asked whether LCN2 overexpression could interfere with the paracrine production of osteoclast-regulating cytokines. In line with this hypothesis, we observed that OBs-LCN2 produced a significantly higher amount of the osteoclastogenic cytokines *RankL* (Fig. 6*A*) and *IL-6* (Fig. 6*B*), and a lower expression of the RANKL decoy receptor *Osteoprotegerin* (*Opg*) (Fig. 6*C*), thus leading to a significant increase of the *RankL*/*Opg* ratio (Fig. 6*D*).

These results prompted us to investigate whether LCN2 could indirectly affect osteoclastogenesis by treating mouse bone marrow mononuclear cells with conditioned media collected from OBs-LCN2 or OBs-empty. This experiment evidenced a significant increase of osteoclast number in the presence of conditioned medium from OBs-LCN2 (Fig. 6*E*). Similar results were observed in purified bone marrow mononuclear cells cocultured with OBs-LCN2 relative to OBs-empty (Fig. 6*F*). This osteoclastogenic effect was not due to the LCN2 itself because the treatment of preosteoclast cultures with rmLCN2 failed to increase osteoclastogenesis over control (Fig. 6*G*).

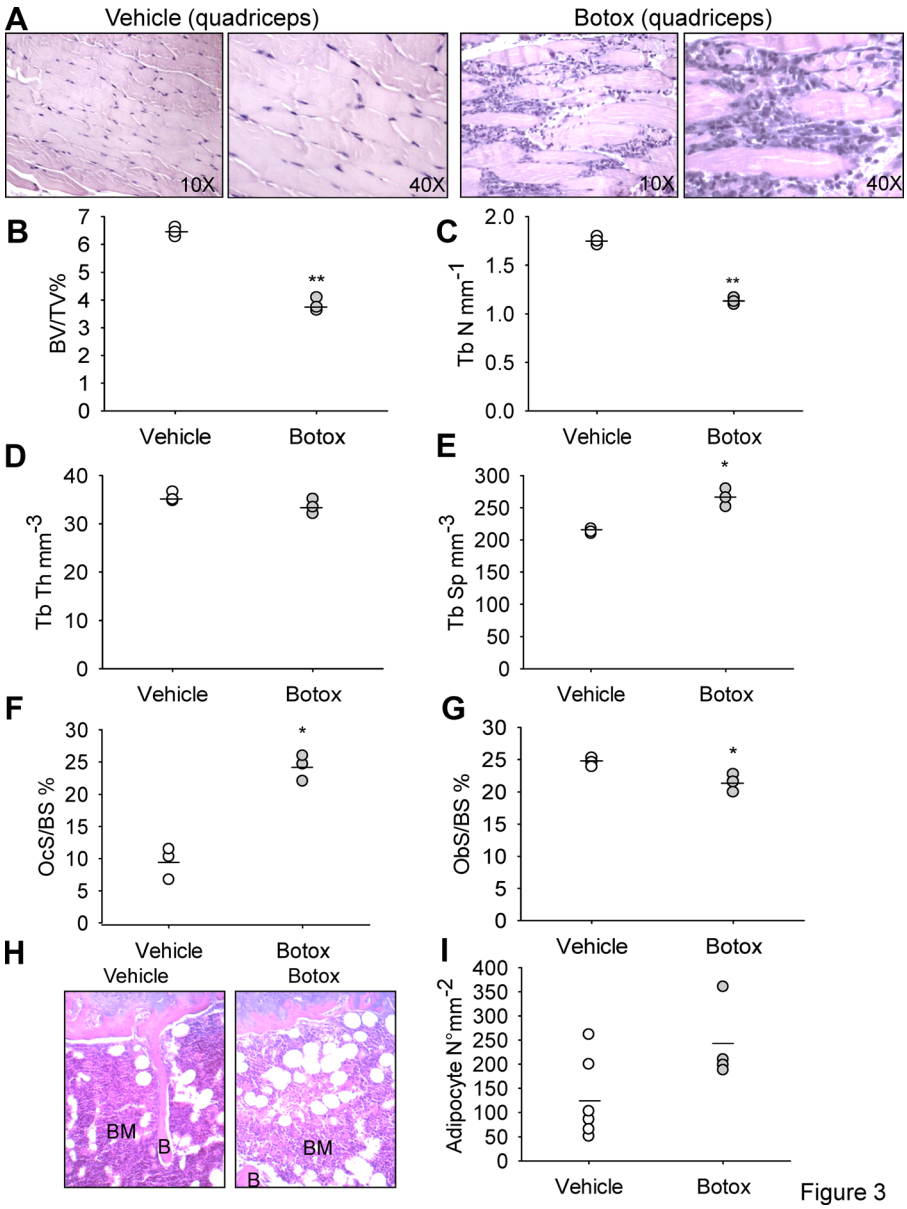

Figure 3

Fig. 3. Effect of transient paralysis on bone phenotype. Eight-week-old mice were injected with saline solution (vehicle) or with Botulin toxin A (Botox, 20 μL of 2.0 unit/100 g), into the right quadriceps and the posterior compartment of the right calf (targeting gastrocnemius, plantaris, and soleus) 4 mm proximal to the patellar tendon of the left or the right hindlimbs, respectively. (*A*) Hematoxylin/eosin staining of muscle sections. (*B–E*) μCT analysis of proximal tibia spongiosa to quantify trabecular (*B*) BV/TV (%), (*C*) Tb.N, (D) Tb.Th, and (*E*) Tb.Sp. (*F*, *G*) Histomorphometric analysis of proximal tibia to quantify (*F*) Oc.S/BS and (*G*) Ob.S/BS. (*H*) Representative picture of femur sections stained with hematoxylin/eosin and (*I*) quantification of the adipocyte number. $^{*}p < 0.03$, $^{**}p = 0.012$ versus vehicle (unpaired *t* test). In *D* and *I* data are statistically not significant, with $p > 0.1$ and $p = 0.17$ versus vehicle, respectively. B = bone; BM = bone marrow; BV/TV = bone volume/total tissue volume; Tb.N = trabecular number; Tb.Th = trabecular thickness; Tb. Sp = trabecular spacing; Oc.S/BS = osteoclast surface/bone surface; Ob.S/BS = osteoblast surface/bone surface.

In order to address whether LCN2 overexpression could induce similar changes in a cell type not correlated with bone, we transfected the human epithelial cell line HEK293 with empty or LCN2-carrying vectors (Fig. 7*A*). Under this condition, increased LCN2 also induced *RankL* mRNA expression (Fig. 7*B*), with albeit no effects on *Opg* expression (Fig. 7*C*). Nevertheless, the *RankL* change led to a significant increase of the *RankL/Opg* ratio (Fig. 7*D*). In contrast, we did not observe any regulation of *IL-6* mRNA level (Fig. 7*E*).

Consistent with the induction of *RankL*, enhanced osteoclast formation was demonstrated in experiments in which purified bone marrow mononuclear cells were cultured in the presence of conditioned medium from HEK293 cells transfected with control or LCN2 vector (Fig. 7*F*). This effect was blunted by treatment with OPG (Fig. 7*G*), confirming that it was due to the increased RANKL concentration in the conditioned medium of LCN2 overexpressing cells.

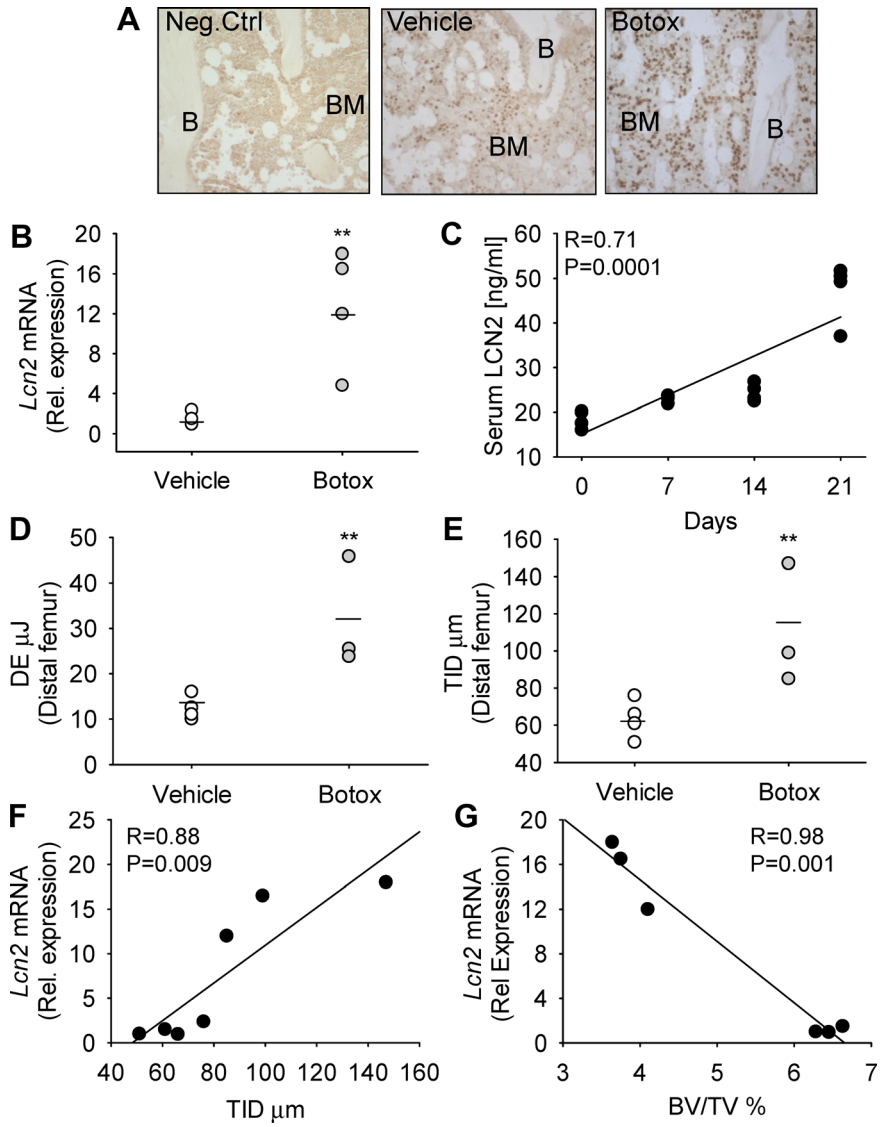

Fig. 4. Effect of transient paralysis on LCN2 transcriptional and protein expression. Right quadriceps of 8-week-old mice injected with saline solution (vehicle) or with Botulin toxin A (Botox, 20 µL of 2.0 unit/100 g). (*A*) Immunocytochemistry for LCN2 detection in tibia sections. (*B*) Transcriptional expression of *Lcn2* by comparative real-time RT-PCR. (*C*) Linear regression test showing a direct correlation between serum LCN2 levels and the duration of unloading. (*D*) Distal femur DE (µJ) and (*E*) TID (µm). (*F*, *G*) Linear regression test showing (*F*) a direct correlation between *Lcn2* mRNA and the TID, and (*G*) an inverse correlation between *Lcn2* mRNA and trabecular bone volume/total tissue volume (BV/TV). $^{**}p < 0.04$ versus vehicle (nonparametric Mann-Whitney rank sum test). B = bone; BM = bone marrow; DE = dissipated energy; TID = total indentation distance.

Discussion

LCN2 is a very versatile molecule that plays different roles in several cell types and conditions. It has recently been the subject of a great interest as an early biomarker not only in renal injury but also in several other conditions, including cancer, anemia, pregnancy, and cardiovascular diseases.[25–28] The multifaceted roles of LCN2 are well evident in tumor cells, where the proposed functions range from inhibiting apoptosis,[29] invasion and angiogenesis,[30] to increasing proliferation and metastasis.[31,32] Ectopic expression of LCN2 also promotes BCR-ABL–induced chronic myelogenous leukemia in murine models.[33] Moreover, it forms a complex with the proteolytic enzyme matrix metalloprotease-9 (MMP-9), thus preventing its degradation.[34]

Despite these many different functions, the role of LCN2 in bone metabolism is still unclear and only recently have some researches begun to elucidate it. Costa and colleagues[35] showed an increased expression of SDF-1 in transgenic mice overexpressing LCN2 specifically in osteoblasts under the control of a type I collagen promoter, that correlated with an increased number of CD34+/CXCR4+ (SDF-1 receptor) cells. These mice also exhibited growth plate defect, reduced bone mass, delayed osteoblast differentiation, and enhanced osteoclast activity, thus supporting our observations.[36] In fact, in our hands, LCN2 appears to have a crucial role, especially in conditions associated

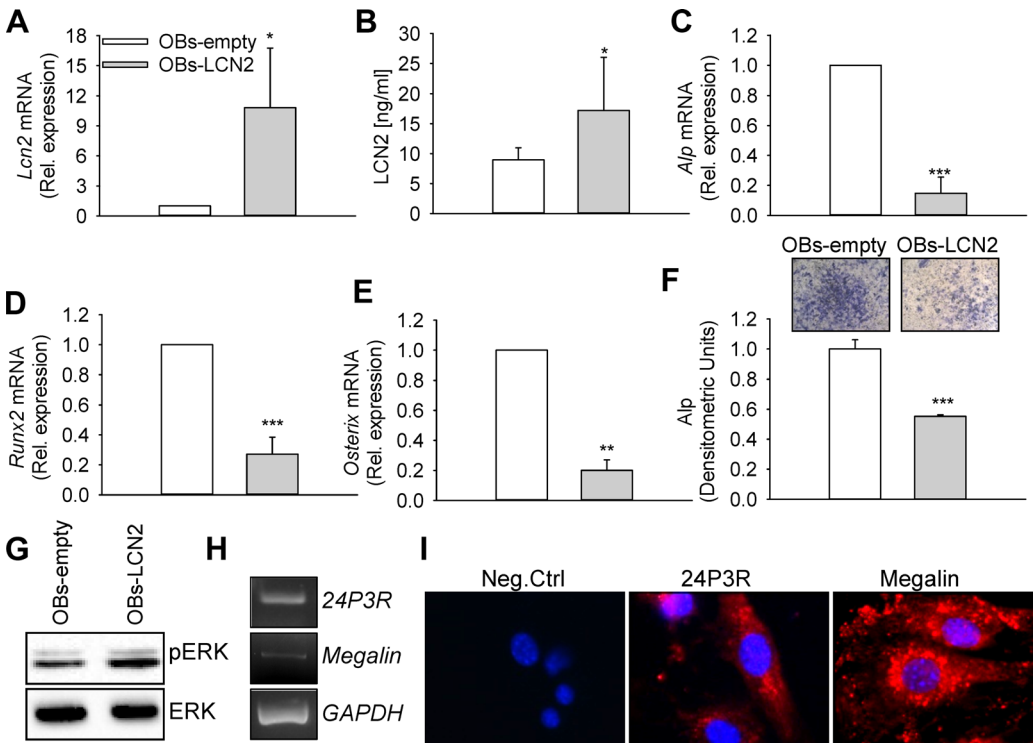

Fig. 5. Effect of LCN2 overexpression on osteoblast differentiation. (*A–F*) Amaxa nucleofection of primary osteoblasts with LCN2 (OBs-LCN2) or with an empty vector as control (OBs-empty). (*A*) mRNA and (*B*) protein expressions of LCN2 performed by comparative real-time RT-PCR and ELISA assays, respectively. (*C–E*) Transcriptional expression of (*C*) *Alp*, (*D*) *Runx2*, and (*E*) *Osterix* by comparative real-time RT-PCR. (*F*) Quantification (graph) of ALP activity evaluated by histochemical assay (inset). (*G*) Western blot analysis of pERK and total ERK. (*H*) mRNA and (*I*) protein expression of the LCN2 receptors, megalin and 24P3R, in primary osteoblasts evaluated by RT-PCR and immunofluorescence, respectively (Neg.Ctrl, immunofluorescence performed by omitting the primary antibody). Data are (*A–F*) the mean ± SD or (*G–I*) representative of three independent experiments. $^{*}p < 0.05$, $^{**}p = 0.038$, and $^{***}p < 0.003$ versus OBs-empty (unpaired *t* test). Neg.Ctrl = negative control; pERK = phosphorylated ERK.

with a decrease of mechanical forces. Our previous work[13] demonstrated that osteoblasts progressively upregulate LCN2 expression in a manner proportional to the reduction of gravitational force intensity. Interestingly, in the present study, we demonstrated a direct correlation between LCN2 serum levels and the mechanical unloading mimicked in human subjects by HDBR conditions. These results were also confirmed in vivo in the long bones of various animal models of mechanical unloading, strongly indicating a causative role of LCN2 in inducing bone loss. Noteworthy, Miravète and colleagues[37] suggested a role of LCN2 in urinary fluid shear stress-induced alterations observed in early phases of most kidney diseases, confirming the mechanoresponding properties of this gene also in another context. Interestingly, our data indicate that increased *Lcn2* expression is specifically associated to unloading-induced bone loss. In fact, contrariwise, in ovariectomized (OVX) mice, which typically reproduce a condition of bone loss independent of mechanical forces, we found a significant reduction of LCN2 compared to sham-operated mice. These data suggest that LCN2 could play an alternative role in postmenopausal osteoporosis, underscoring the need of further work to deeply understand its complex involvement in the context of bone metabolism.

Mechanistically, in vivo $CD45^{-}$cells, known to belong to the stromal cellular component of the bone marrow that also includes the osteoblast lineage, were the major sources of LCN2 in unloading conditions. Furthermore, increased LCN2 levels matched with an inhibition of osteoblast differentiation, as demonstrated by our in vitro study, where the overexpression of LCN2 alone in osteoblasts sufficed to inhibit their differentiation. In fact, crucial osteoblast genes such as *Runx2*, *Osterix*, and *Alp*, which were previously noted to be downregulated under reduced mechanical forces in vitro,[13] were blunted in osteoblasts overexpressing LCN2. Our results also suggest that LCN2 works upstream of the typical osteoblast master protein, Runx2, representing a novel primary osteoblast differentiation regulatory pathway.

Interestingly, LCN2 also appears to contribute to the osteoblast-osteoclast coupling. In fact, overexpression of LCN2 in osteoblasts increased their ability to stimulate osteoclastogenesis through the induction of the pro-osteoclastogenic factors, RANKL and IL-6, and the inhibition of the anti-osteoclastogenic factor, OPG. The induction of RANKL by LCN2 was observed also in a bone-unrelated cell line (HEK293). Consistently, HEK293 cell conditioned medium had pro-osteoclastogenic properties fully blocked by treatment with the RANKL-decoy receptor, OPG. In contrast, LCN2 did not exhibit pro-osteoclastogenic properties itself, suggesting a dominant role only in osteoblasts, which reliably expressed both LCN2 receptors, megalin and 24P3R, and responded to LCN2 overexpression through the ERK pathway.

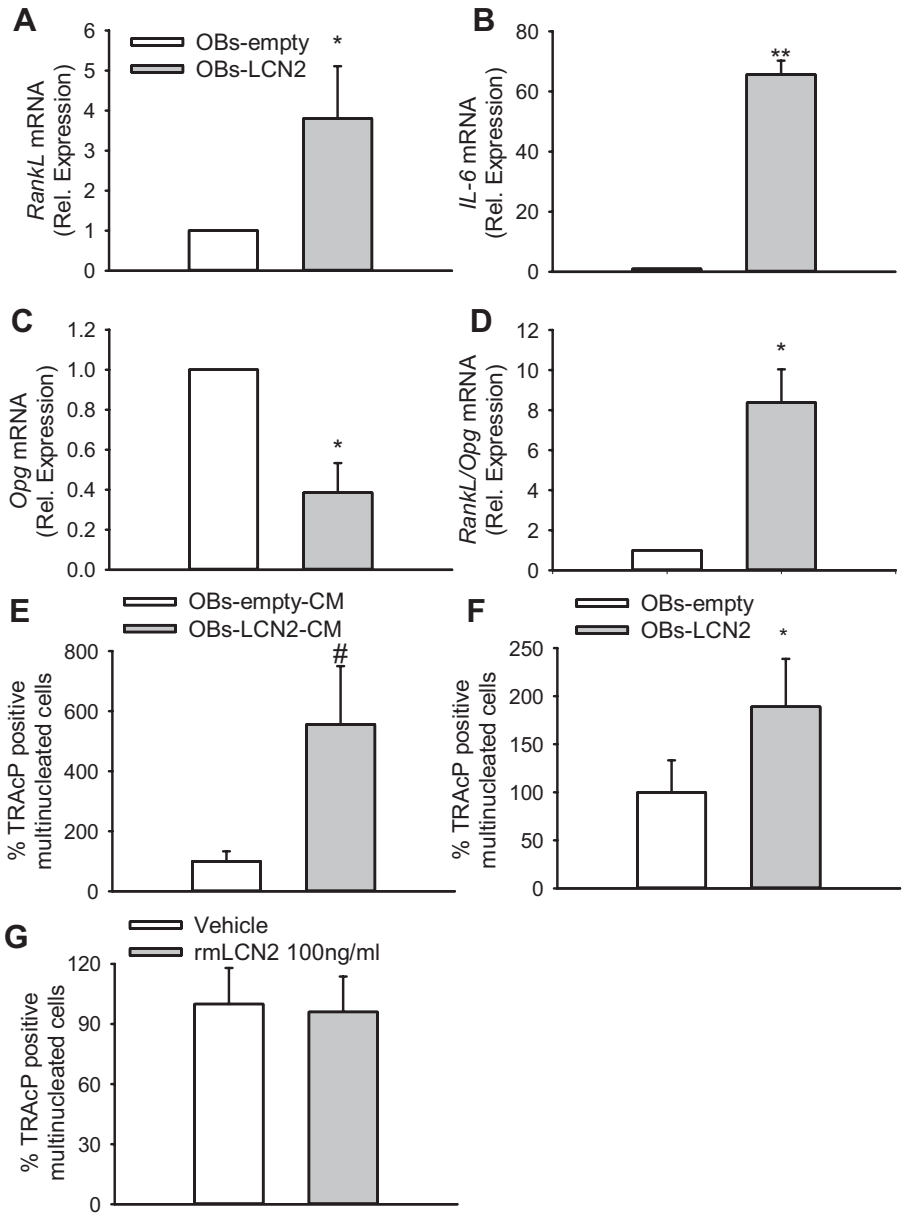

Fig. 6. Effect of LCN2 overexpression on osteoclastogenesis. (*A–D*) RNA from osteoblasts transfected with LCN2 (OBs-LCN2) or with the empty vector (OBs-empty) was extracted, retro-transcribed, and subjected to comparative real-time RT-PCR for (*A*) *RankL*, (*B*) *IL-6*, and (*C*) *Opg* mRNAs evaluation. Data are normalized versus the housekeeping gene *Gapdh*. (*D*) *RankL/Opg* ratio. (*E*) Purified bone marrow mononuclear cells were treated with CM from osteoblasts transfected with LCN2 (OBs-LCN2-CM) or with the empty vector (OBs-empty-CM) in the presence of M-CSF and suboptimal concentrations of RANKL for 7 days. (*F*) OBs-empty and OBs-LCN2 cells were cocultured with purified mouse bone marrow mononuclear cells for 7 days. (*G*) Purified bone marrow mononuclear cells were treated with rmLcn2 (100 ng/mL). At the end of the experiment, mature osteoclasts were detected by TRAcP histochemical staining. Results are the mean ± SD of three independent experiments. $^{*}p < 0.02$ and $^{**}p = 0.0026$ versus OBs-empty; $\#p = 0.0028$ versus OBs-empty-CM; in (*F*) $p = 0.06$ versus OBs-empty (unpaired *t* test). CM = conditioned media; TRAcP = tartrate-resistant acid phosphatase.

In conclusion, we believe that LCN2 is an important osteoblast mechanoresponding gene with a role in bone metabolism, that could be involved in the onset of osteoporosis induced by mechanical failures due for instance to disuse, bed rest, muscle impairment or aging, decreasing osteoblast differentiation, and increasing osteoblast-induced osteoclastogenesis. These results open a new perspective in the understanding of the molecular mechanisms governing bone metabolism under stimulation by mechanical forces in physiologic and pathologic conditions, and establish a track for diagnostic and therapeutic developments also in humans.

Disclosures

All authors state that they have no conflicts of interest.

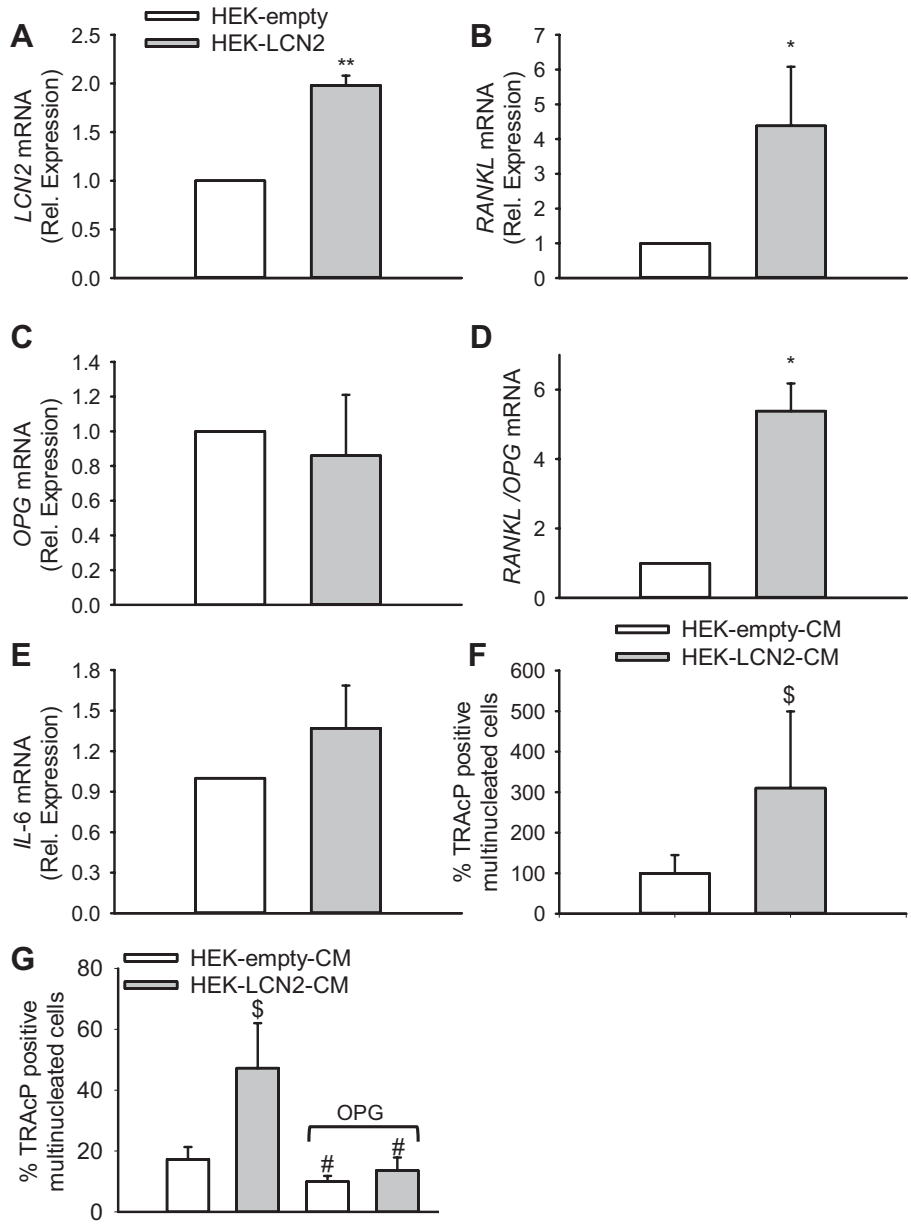

Fig. 7. LCN2 overexpression in HEK293 cells. HEK293 cells were transfected with an empty vector (HEK-empty) or with a construct carrying LCN2 (HEK-LCN2). (A-E) Cells were collected, the RNA was extracted, reverse-transcribed, and subjected to comparative real-time RT-PCR, using primer pairs and conditions specific for (*A*) *Lcn2*, (*B*) *RankL*, and (*C*) *Opg*. In (*D*) the *Rankl/Opg* ratio was calculated (E) Comparative real-time RT-PCR using primer pairs and conditions specific for *IL-6*. Results are reported as fold increase and are normalized versus the housekeeping gene *GAPDH*. (*F*) hPBMCs obtained by Ficoll separation were allowed to differentiate into osteoclasts in the presence of M-CSF, suboptimal concentrations of RANKL and conditioned media from HEK293 cells transfected with empty vector (HEK-empty-CM) or with LCN2 (HEK-LCN2-CM). (*G*) hPBMCs, were allowed to differentiate into osteoclasts as described in *F*, with or without OPG. Data are the mean ± SD of three independent experiments. $^{*}p < 0.05$ and $^{**}p < 0.005$ versus HEK-empty; $^{\$}p < 0.05$ versus HEK-empty-CM and $\#p < 0.04$ versus HEK-empty-CM and HEK-LCN2-CM (unpaired *t* test). hPBMC = human peripheral blood mononuclear cell; OPG = osteoprotegerin; CM = conditioned media.

Acknowledgments

This work was supported by the STRODER-SIOMMMS grant to NR, by a grant from the "Agenzia Spaziale Italiana" (ASI) to AT, by the DLR Space Programme to MH and by the European Union grant SYBIL - FP7-HEALTH-2013-INNOVATION - 602300. We are indebted with Dr. Rita Di Massimo for her excellent contribution in writing this manuscript.

Authors' roles: Study design: NR, MC, and AT. Study conduct: NR, MC, AC, SGP, PL, PFM, MH, and AT. Data collection: NR, MC, AC, and AT. Data analysis: NR, MC, AC, and AT. Data interpretation: NR, MC, and AT. Drafting manuscript: NR and AT. Revising manuscript content: NR, MC, and AT. Approving final version of manuscript: NR, MC, AC, SGP, PL, PFM, MH, and AT. NR takes responsibility for the integrity of the data analysis.

References

1. Kjeldsen L, Johnsen AH, Sengelov H, Borregaard N. Isolation and primary structure of NGAL, a novel protein associated with human neutrophil gelatinase. J Biol Chem. 1993;268:10425–32.
2. Kjeldsen L, Bainton DF, Sengelov H, Borregaard N. Identification of neutrophil gelatinase-associated lipocalin as a novel matrix protein of specific granules in human neutrophils. Blood. 1994;83:799–807.
3. Goetz DH, Holmes MA, Borregaard N, Bluhm ME, Raymond KN, Strong RK. The neutrophil lipocalin NGAL is a bacteriostatic agent that interferes with siderophore-mediated iron acquisition. Mol Cell. 2002;10:1033–43.
4. Flo TH, Smith KD, Sato S, et al. Lipocalin 2 mediates an innate immune response to bacterial infection by sequestrating iron. Nature. 2004;32:917–21.
5. Berger T, Togawa A, Duncan GS, et al. Lipocalin 2-deficient mice exhibit increased sensitivity to Escherichia coli infection but not to ischemia-reperfusion injury. Proc Natl Acad Sci U S.A. 2006;103:1834–9.
6. Wang Y, Lam KS, Kraegen EW, et al. Lipocalin-2 is an inflammatory marker closely associated with obesity, insulin resistance, and hyperglycemia in humans. Clin Chem. 2007;53:34–41.
7. Yan QW, Yang Q, Mody N, et al. The adipokine lipocalin 2 is regulated by obesity and promotes insulin resistance. Diabetes. 2007;56:2533–40.
8. Choi KM, Lee JS, Kim EJ, et al. Implication of lipocalin-2 and visfatin levels in patients with coronary heart disease. Eur J Endocrinol. 2008;158:203–7.
9. Schmidt-Ott KM, Mori K, Kalandadze A, et al. Neutrophil gelatinase associated lipocalin-mediated iron traffic in kidney epithelia. Curr Opin Nephrol Hypertens. 2006;15:442–9.
10. Devireddy LR, Gazin C, Zhu X, Green MR. A cell-surface receptor for lipocalin 24p3 selectively mediates apoptosis and iron uptake. Cell. 2005;123:1293–305.
11. Hvidberg V, Jacobsen C, Strong RK, Cowland JB, Moestrup SK, Borregaard N. The endocytic receptor megalin binds the iron transporting neutrophil-gelatinase-associated lipocalin with high affinity and mediates its cellular uptake. FEBS Lett. 2005;579:773–7.
12. Mori K, Lee HT, Rapoport D, et al. Endocytic delivery of lipocalin-siderophore-iron complex rescues the kidney from ischemia-reperfusion injury. J Clin Invest. 2005;115:610–21.
13. Capulli M, Rufo A, Teti A, Rucci N. Global transcriptome analysis in mouse calvarial osteoblasts highlights sets of genes regulated by modeled microgravity and identifies a "mechanoresponsive osteoblast gene signature." J Cell Biochem. 2009;107:240–52.
14. Frings-Meuthen P, Buehlmeier J, Baecker N, et al. High sodium chloride intake exacerbates immobilization-induced bone resorption and protein losses. J Appl Physiol. 2011;111:537–42.
15. Sakata T, Sakai A, Tsurukami H, et al. Trabecular bone turnover and bone marrow cell development in tail-suspended mice. J Bone Miner Res. 1999;14:1596–604.
16. Warner SE, Sanforda DA, Beckera BL, Bainb SD, Srinivasana S, Grossa TS. Botox induced muscle paralysis rapidly degrades bone. Bone. 2006;38:257–64.
17. Bulfield G, Siller WG, Wight PA, Moore KJ. X chromosome-linked muscular dystrophy (mdx) in the mouse. Proc Natl Acad Sci U S A. 1984;81:1189–92.
18. Rufo A, Del Fattore A, Capulli M, et al. Mechanisms inducing low bone density in Duchenne muscular dystrophy in mice and humans. J Bone Miner Res. 2011;26:1891–03.
19. Goes ATR, Souza LC, Filho CB, et al. Neuroprotective effects of swimming training in a mouse model of Parkinson's disease induced by 6-hydroxydopamine. Neuroscience. 2014;256:61–71.
20. Lorensen WE, Cline HE. Marching cubes: a high resolution 3D surface construction algorithm. Comput Graphics. 1987;21:163–9.
21. Bouxsein ML, Boyd SK, Christiansen BA, Guldberg RE, Jepsen KJ, Müller R. Guidelines for assessment of bone microstructure in rodents using micro-computed tomography. J Bone Miner Res. 2010;25:1468–86.
22. Rucci N, Rufo A, Alamanou M, et al. The glycosaminoglycan-binding domain of PRELP acts as a cell type-specific NF-kappaB inhibitor that impairs osteoclastogenesis. J Cell Biol. 2009;187:669–83.
23. Dempster DW, Compston JE, Drezner MK, et al. Standardized nomenclature, symbols, and units for bone histomorphometry: a 2012 update of the report of the ASBMR Histomorphometry Nomenclature Committee. J Bone Miner Res. 2013;28:2–17.
24. Rucci N, Rufo A, Alamanou M, Teti A. Modeled microgravity stimulates osteoclastogenesis and bone resorption by increasing osteoblast RANKL/OPG ratio. J Cell Biochem. 2007;100:464–73.
25. Makris K, Rizos D, Kafkas N, Haliassos A. Neurophil gelatinase-associated lipocalin as a new biomarker in laboratory medicine. Clin Chem Lab Med. 2012;50:1519–32.
26. Bolignano D, Donato V, Lacquaniti A, et al. Neutrophil gelatinase-associated lipocalin (NGAL) in human neoplasias: a new protein enters the scene. Cancer Lett. 2010;288:10–6.
27. Huang HL, Chu ST, Chen YH. Ovarian steroids regulate 24p3 expression in mouse uterus during the natural estrous cycle and the preimplantation period. J Endocrinol. 1999;162:11–9.
28. D'Anna R, Baviera G, Corrado F, Giordano D, Recupero S, Di Benedetto A. First trimester serum neutrophil gelatinase-associated lipocalin in gestational diabetes. Diabet Med. 2009;26:1293–5.
29. Iannetti A, Pacifico F, Acquaviva R, Lavorgna A, Crescenzi E, Vascotto C. The neutrophil gelatinase-associated lipocalin (NGAL), a NF-kappaB-regulated gene, is a survival factor for thyroid neoplastic cells. Proc Natl Acad Sci U S A. 2008;105:14058–63.
30. Moniaux N, Chakraborty S, Yalniz M, et al. Early diagnosis of pancreatic cancer: neutrophil gelatinase associated lipocalin as a marker of pancreatic intraepithelial neoplasia. Br J Cancer. 2008;98:1540–7.
31. Sun Y, Yokoi K, Li H, et al. NGAL expression is elevated in both colorectal adenoma-carcinoma sequence and cancer progression and enhances tumorigenesis in xenograft mouse models. Clin Cancer Res. 2011;17:4331–40.
32. Bauer M, Eickhoff JC, Gould MN, Mundhenke C, Maass N, Friedl A. Neutrophil gelatinase-associated lipocalin (NGAL) is a predictor of poor prognosis in human primary breast cancer. Breast Cancer Res Treat. 2008;108:389–97.
33. Leng X, Lin H, Ding T, et al. Lipocalin 2 is required for BCR-ABL-induced tumorigenesis. Oncogene. 2008;27:6110–9.
34. Yan L, Borregaard N, Kjeldsen L, Moses MA. The high molecular weight urinary matrix metalloproteinase (MMP) activity is a complex of gelatinase B/MMP-9 and neutrophil gelatinase-associated lipocalin (NGAL). Modulation of MMP-9 activity by NGAL. J Biol Chem. 2001;276:37258–65.
35. Costa D, Biticchi R, Negrini S, et al. Lipocalin-2 controls the expression of SDF-1 and the number of responsive cells in bone. Cytokine. 2010;51:47–52.
36. Costa D, Lazzarini E, Canciani B, et al. Altered bone development and turnover in transgenic mice over-expressing lipocalin-2 in bone. J Cell Physiol. 2013;228:2210–21.
37. Miravète M, Dissard R, Klein J, et al. Renal tubular fluid shear stress facilitates monocyte activation toward inflammatory macrophages. Am J Physiol Renal Physiol. 2012;302:F1409–7.